

# Virtual Full-Duplex Cooperative NOMA: Relay Selection and Interference Cancellation

Young-Bin Kim, *Member, IEEE*, Kosuke Yamazaki, and Bang Chul Jung<sup>✉</sup>, *Senior Member, IEEE*

**Abstract**—In this paper, we propose a *virtual full-duplex cooperative non-orthogonal multiple access (NOMA) framework for a downlink two-hop network assisted by multiple half-duplex decode-and-forward (DF) relay stations (RSs)*. In the proposed virtual full-duplex framework, the RSs except for a selected RS to forward the received signal suffer from inter-RS interference since both the BS and the selected RS transmit the super-imposed signal simultaneously. To address this problem, we propose an RS selection algorithm with adaptive inter-RS interference management and we mathematically attain the closed-form outage probability, which is challenging in general. In addition, we investigate diversity-multiplexing tradeoff (DMT) performance of a modified version of the proposed RS selection algorithm based on a discrete Markov chain, which adaptively resets the successive transmission. Simulation results show that the proposed RS selection algorithm outperforms the conventional cooperative NOMA algorithm in terms of both the outage probability and the DMT, which has the best performance reported in the literature.

**Index Terms**—Non-orthogonal multiple access (NOMA), virtual full-duplex, cooperative NOMA relay selection, outage probability, diversity-multiplexing tradeoff (DMT).

## I. INTRODUCTION

NON-ORTHOGONAL multiple access (NOMA) is considered a promising candidate of 5G technologies [1] to satisfy the performance requirements of 5G including massive connectivity, low latency, and high spectral efficiency [2]. The basic idea of NOMA is to simultaneously support multiple signals of users in a single signal domain, *i.e.*, a power or code domain. Code domain based NOMA exploits a unique spreading code for each user, whereas power domain based NOMA allocates different power to each user's component signal which is linearly combined to each other's composite signal. The power allocated to the composite signals can be determined according to the channel gain of

the users [3], [4] or the required quality-of-service (QoS) of users [5].<sup>1</sup>

In addition to the conventional NOMA techniques, several *cooperative NOMA* systems that exploit additional spatial diversity from half-duplex relay stations (RSs) have been proposed [6]–[13]. In [8], [10], and [11], a single RS was considered between transmitters and receivers. The NOMA system with a single amplify-and-forward (AF) relaying was investigated over Nakagami- $m$  fading channels [8] and Rayleigh fading channels [11], where it was shown that the cooperative NOMA outperforms the orthogonal multiple access (OMA) in terms of both outage probability and systemic throughput. In [10], the cooperative NOMA with a half-duplex DF RS was proposed for a network consisting of two sources, two users, and a single shared relay, and analyzed in terms of ergodic sum capacity with perfect and imperfect successive interference cancellation (SIC).

On the other hand, multiple RSs were considered between transmitters and receivers in [6], [7], [9], [12], and [13]. In [6], a coordinated direct and relay transmission (CDRT) technique was proposed for downlink NOMA systems, where the BS directly sends data to the user with a relatively better channel condition (*i.e.*, cell-center user) while communicating with a user that has relatively poor channel conditions (*i.e.*, cell-edge user) only through a relay. In particular, in [6], the RS only sends data of the cell-edge user in the second hop, while the BS sends data of both users at the same time. In [7], a two-stage RS selection technique was proposed for the downlink NOMA systems and its performance was analyzed in terms of outage probability, where it is assumed that there exists no direct link from the BS to two mobile stations (MSs). Thus, the BS sends data for two MSs to multiple RSs at the first transmission phase, and one of the RSs is selected to send the data to two MSs at the second transmission phase. In [9], another cooperative NOMA technique was proposed in the downlink cellular network which consists of a BS, two MSs, and two RSs, where the first RS is for the first MS and the second RS is for the second MS. In the first transmission phase, the BS sends data of two MSs to two RSs, and two RSs simultaneously send data of two MSs [9]. At the second transmission phase, dirty paper coding (DPC) technique was adopted to precode signals at each RS in order to cancel out the inter-RS interference [9]. In [12], a relay-aided

Manuscript received March 14, 2019; revised July 21, 2019; accepted August 26, 2019. Date of publication September 16, 2019; date of current version December 10, 2019. This work was supported by the NRF through the Basic Science Research Program funded by the Ministry of Science and ICT under Grant NRF2019R1A2B5B01070697. The associate editor coordinating the review of this article and approving it for publication was M. Xiao. (*Corresponding author: Bang Chul Jung.*)

Y.-B. Kim was with KDDI Research, Inc., Saitama 356-8502, Japan. He is now with Rakuten Mobile, Inc., Tokyo 158-0096, Japan (e-mail: youngbin.kim@rakuten.com).

K. Yamazaki is with KDDI Research, Inc., Saitama 356-8502, Japan (e-mail: ko-yamazaki@kddi-research.jp).

B. C. Jung is with the Department of Electronics Engineering, Chungnam National University, Daejeon 34134, South Korea (e-mail: bcjung@cnu.ac.kr).

Color versions of one or more of the figures in this article are available online at <http://ieeexplore.ieee.org>.

Digital Object Identifier 10.1109/TWC.2019.2940220

<sup>1</sup>The motivation for our work corresponds with the latter case. To be more specific, the target rates of the users are different from each other where their average channel gains are the same, which has been considered for NOMA in [5] and [7] as well.

NOMA technique was proposed for multi-cell uplink cellular networks in which each cell supports  $K$  single-antenna users, where an Alamouti structure was adopted for the desired symbol, resulting in diversity gain of two. The achievable rate of a cooperative NOMA technique was mathematically analyzed in the downlink using efficient approximation via Gauss-Chebyshev integration in Rician fading environments [13].

The above-mentioned studies, however, inherently suffer from a multiplexing loss since half-duplex RSs cannot transmit and receive simultaneously. Hence, at least two transmission phases are required to transmit a signal to users in the absence of channels between a BS and users. Recently, NOMA-based schemes with a *full-duplex* RS have been proposed in order to overcome this problem [14]–[23]. A compress-and-forward (CF)-based full-duplex relay was proposed for the downlink cooperative NOMA system [14], where the achievable rate region of the proposed technique was analyzed. In [15], a full-duplex NOMA system was considered for a downlink cellular network consisting of a BS, two users, and a dedicated full-duplex relay for a cell-edge user. Under the realistic assumption of imperfect self-interference cancellation at the full-duplex relay, the outage probability of both users and the ergodic sum capacity were analyzed. A full-duplex device-to-device (D2D)-aided cooperative NOMA system was proposed for the downlink cellular network, where a cell-center user operates with full-duplex and helps a cell-edge user [16]. In [17], a cell-center user operates as a full-duplex relay for a cell-edge user as in [16]. In particular, the closed-form expression of outage probability and ergodic sum rate were analyzed and the optimal power allocation rule was derived for maximizing the minimum achievable rates of users or minimizing the outage probability [17]. In [18], a NOMA-based multi-pair two-way full-duplex relay network was studied where a rate splitting scheme and a successive group decoding strategy were proposed. A NOMA cognitive radio network was considered, where a multi-antenna full-duplex relay assists transmission from a BS to a cognitive cell-edge user, while the BS transmits to a cognitive cell-center at the same time [19]. In particular, a joint beamforming and power allocation technique was proposed for the full-duplex relay to improve the system performance. In [20], the merits of the multi-antenna full-duplex RS was analyzed under the assumption of imperfect self-interference and inter-relay interference cancellation. By exploiting the beamformers in order to null out the self-interference at the RS, the authors of [20] showed the performance improvement in terms of outage probability compared to the two-hop half-duplex operation. Cooperative NOMA based full-duplex RS was proposed to cope with simultaneous wireless information and power transfer (SWIPT) based networks [21] and self-backhauling heterogeneous networks [22].

Even though there are many studies on full-duplex relays in the literature, perfect self-interference cancellation as well as cost-effective implementation thereof are still challenging in practice. A number of studies have dealt the effect of imperfect self-interference cancellation in the full-duplex relaying techniques [20]–[22]. In the view of actual applications, integrated access and backhaul (IAB) are an example that we still need to

consider the half-duplex operation at relays. IAB is a practical application candidate in 5G in order to compensate for the relatively narrow coverage of mmWave systems by using the multi-hop half-duplex relaying techniques reported in [24] and [25]. Moreover, the hardware complexity of the self-interference canceller is still a challenging issue in the view of practicality even for a moderate number of antennas [26]. In this regard, we cannot confirm that the full-duplex operation always outperforms the half-duplex operation in relays. Thus, it is necessary to resolve the multiplexing loss suffering from half-duplex (multi-hop) relaying via other practical techniques.

In this paper, we propose a novel spectrally-efficient cooperative NOMA technique for a two-hop downlink cellular network that consists a single BS, two MSs, and  $K$  half-duplex RSs in the absence of the direct link from the BS to two MSs. The proposed technique compensates for the multiplexing loss due to the half-duplex operation of multiple RSs via successive relaying operation of *a selected* RS as in [27] and [28], which is called *virtual full-duplex (VFD)* cooperative NOMA. We also mathematically analyze the performance of the proposed technique in terms of outage probability, and compare it with that of the conventional cooperative NOMA technique [7] that has been proposed in the same system model and known to result in the best performance in the literature. Based on the mathematical analysis, we further analyze the proposed technique in terms of diversity-multiplexing tradeoff (DMT), and show that the proposed technique also outperforms the conventional techniques in terms of DMT. Note that the proposed relay selection technique operates in a distributed manner with a finite amount of feedback and it can be easily implemented in practical cellular networks. As for the novelty of our work, the proposed technique is not a simple extension of the existing study in [7], even though it is proposed in the same network model as [7]. By allowing for both the BS and RSs to send their signals simultaneously, i.e., virtual full-duplex operation, fundamental throughput improvement can be achieved and a new type of interference, inter-relay interference, is induced. We also rigorously analyze the proposed technique in terms of outage probability and DMT which are the most reliable and convincing performance metrics in the literature. Those performance metrics are in general difficult to analyze.

The rest of this paper is organized as follows. In Section II, we describe the system model considered in this paper. The virtual full-duplex cooperative NOMA technique is proposed in Section III. The outage probability of the proposed technique is analyzed using the discrete Markov chain in Section IV. The DMT of the proposed technique is analyzed in Section V. Numerical results are shown in Section VI and conclusions are drawn in Section VII.

## II. SYSTEM MODEL

We consider a single-cell downlink network consisting of a single BS, two MSs, and  $K$  half-duplex decode-and-forward (DF) relay stations (RSs) as depicted in Fig. 1. Each node is assumed to be equipped with a single antenna, and we assume there is no direct link between the BS and two MSs as in [7] and [9]. In this paper, we assume a virtual full-duplex

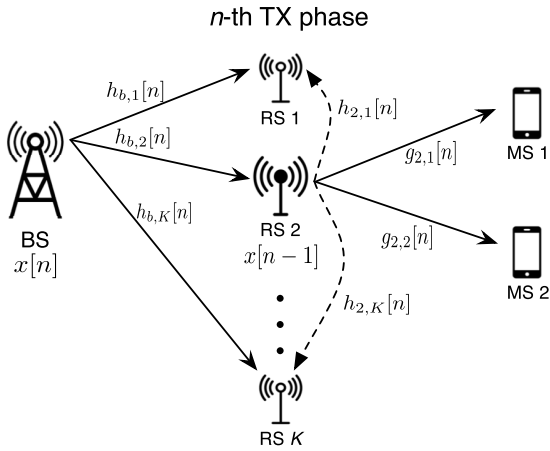


Fig. 1. A two-hop single-cell downlink network with  $K$  half-duplex relays.

operation at the RSs, in which a particular RS sends a packet while the other RSs receive a packet from the BS at the same time. Specifically, The number of total successive transmission phases is assumed to be  $N$ . The received signal at the  $k$ -th RS in the  $n$ -th transmission phase is given by

$$y_k^r[n] = h_{b,k}[n]x[n] + h_{j,k}[n]x[n-1] + z_k^r[n], \quad (1)$$

where  $x[n]$  and  $h_{b,k}[n]$  denote the signal transmitted from the BS in the  $n$ -th transmission phase and the channel coefficient from the BS to the  $k$ -th RS in the  $n$ -th phase, respectively ( $1 \leq k \leq K$ ,  $1 \leq n \leq N$ ). Note that  $x[0] = 0$ . We assume that  $h_{b,k}[n]$  is an i.i.d. complex Gaussian random variable, i.e.,  $h_{b,k}[n] \sim \mathcal{CN}(0,1)$  and  $z_k^r[n]$  represents the thermal noise at the  $k$ -th RS in the  $n$ -th phase, which follows an i.i.d. complex Gaussian distribution, i.e.,  $z_k^r[n] \sim \mathcal{CN}(0, N_0)$ . We assume that  $\mathbb{E}[|x[n]|^2] = P$ , and then the average SNR is given by  $\rho = P/N_0$ . In (1), without loss of generality, we assume that the  $j$ -th RS ( $j \neq k$ ) is chosen to send the  $(n-1)$ -th packet to two MSs and  $h_{j,k}$  denotes the channel coefficient from the  $j$ -th RS to the  $k$ -th RS, which is also an i.i.d. complex Gaussian random variable, i.e.,  $h_{j,k}[n] \sim \mathcal{CN}(0,1)$ . In NOMA, the BS sends the superimposed signal that is given by  $x[n] = \sqrt{a_1}s_1[n] + \sqrt{a_2}s_2[n]$ , where  $s_i[n]$  and  $\sqrt{a_i}$  denote the desired signal of the  $i$ -th MS in the  $n$ -th phase and the power allocation coefficient for the  $i$ -th MS ( $a_1 + a_2 = 1$ ), respectively.

Let  $\mathcal{D}[n]$  be the index set of the RSs that successfully decode the  $n$ -th packet from the BS during the  $n$ -th transmission phase. Then,  $|\mathcal{D}[n]|$  indicates the cardinality of the decoding set. A RS among the RSs included in  $\mathcal{D}[n-1]$  is selected to send the decoded packet to two MSs in the  $n$ -th transmission phase. Thus, in (1), the  $j$ -th RS is assumed to succeed to decode the  $(n-1)$ -th packet from the BS, i.e.,  $j \in \mathcal{D}[n-1]$ . The RS selection algorithm is explained in the next section.

At the  $i$ -th MS, the received signal is given by

$$y_i^m[n] = g_{j,i}[n]x[n-1] + z_i^m[n], \quad (2)$$

where  $g_{j,i}[n]$  denotes the channel coefficient from the  $j$ -th RS to the  $i$ -th MS ( $i = 1, 2$ ), which is an i.i.d. complex Gaussian random variable, i.e.,  $g_{j,i}[n] \sim \mathcal{CN}(0,1)$ , and  $x[n-1]$  denotes

the  $(n-1)$ -th packet from the BS. At RSs, we also assume that  $\mathbb{E}[|x[n-1]|^2] = P$  and  $z_i^m[n]$  represents the thermal noise at the  $i$ -th MS in the  $n$ -th phase, which follows an i.i.d. complex Gaussian distribution, i.e.,  $z_i^m[n] \sim \mathcal{CN}(0, N_0)$ .

We assume that two MSs are categorized not by channel quality but by different QoS requirements as in [7]. In this paper, perfect CSI at the receiver (CSIR) is assumed. Since the CSIR is relatively easy to obtain through the pilot signals embedded to data signals in general, the CSIR as well as the time and energy for obtaining it are explicitly or implicitly assumed in many academic papers including [2]–[14]. Throughout this paper, the priority of the first MS is assumed to be higher than that of the second MS. Dynamic power allocation strategies in each transmission phase may improve the performance, but they are outside the scope of this paper. Hence, we assume that  $a_1$  and  $a_2$  are fixed over  $N$  transmission phases.

### III. VIRTUAL FULL-DUPLEX COOPERATIVE NOMA

The BS broadcasts the superposed signals for two MSs in each transmission phase except for the last transmission phase (i.e.,  $n = N$ ) in order to overcome the throughput loss due to half-duplex operation of RSs. Meanwhile, a selected RS among which RSs successfully decode the received packet from the BS in the previous transmission phase (i.e.,  $k \in \mathcal{D}[n-1]$ ) forwards the packet to the MSs. Hence,  $N-1$  packets are sent to two MSs from the BS during  $N$  transmission phases in the proposed VFD cooperative NOMA. Transmissions at each node are assumed to be synchronized as done in various studies in the literature [6], [8]–[17], [27], [28]. In this section, we first investigate conditions for the successful decoding of the received packet at the RSs, and then describe the proposed relay selection algorithm.

#### A. Conditions for Successful Decoding at RSs

When the decoding set is empty, i.e.,  $|\mathcal{D}[n-1]| = 0$ , the conditions for the  $k$ -th RS to successfully decode the received signals,  $s_1[n]$  and  $s_2[n]$ , at the  $n$ -th transmission phase are given by

$$(C1): \log\left(1 + \frac{a_1 |h_{b,k}[n]|^2}{a_2 |h_{b,k}[n]|^2 + 1/\rho}\right) \geq \frac{NR_1}{N-1}, \quad (3)$$

$$(C2): \log\left(1 + a_2 \rho |h_{b,k}[n]|^2\right) \geq \frac{NR_2}{N-1}, \quad (4)$$

where  $R_1$  and  $R_2$  denote the target rate for the first and second MSs, respectively. Note that (3) and (4) represents the conditions of successful decoding at RSs when there is no inter-RS interference signals. At the first transmission phase, these conditions are used at RSs since  $|\mathcal{D}[0]| = 0$ .

When inter-RS interference exists, i.e.,  $|\mathcal{D}[n-1]| \neq 0$ , all RSs except for the selected RS suffer from interference signals from the selected RS at the  $n$ -th transmission phase. In this case, the conditions for the successful decoding at the RS depend on whether it is included in the previous decoding set. If the  $k$ -th RS is not selected to relay signals to MSs and belongs to the previous decoding set, i.e.,  $k \in \mathcal{D}[n-1]$ , then the conditions for the successful decoding are the same

as (3) and (4) because it already has the interference signals from the selected RS and knows the channel coefficient from the selected RS to itself by the assumption of local CSI.

On the other hand, if  $k \notin \mathcal{D}[n-1]$ , then the  $k$ -th RS tries to perform joint decoding of both the  $n$ -th desired signal from the BS and the  $(n-1)$ -th interference signal from the selected RS rather than the successive interference cancellation strategy since the JD strategy outperforms the SIC in multiple access channels (MACs) in general [29]. In this case, a multiple-access channel (MAC) becomes formed at the RSs except for the selected RS, consisting of the BS (superposed desired signals) and the selected RS (superposed interference signals). In order to obtain the conditions for successful decoding of the  $n$ -th transmission phase at the  $k$ -th RS such that  $k \notin \mathcal{D}[n-1]$ , we need to investigate the achievable rate region of the MAC channel consisting of four signals such as  $\sqrt{a_1}s_1[n-1]$ ,  $\sqrt{a_2}s_2[n-1]$ ,  $\sqrt{a_1}s_1[n]$ , and  $\sqrt{a_2}s_2[n]$ . As in (1), we assume that the  $j$ -th RS sends the  $(n-1)$ -th packet to two MSs ( $j \neq k$ ). Then,  $\sqrt{a_1}s_1[n-1]$  and  $\sqrt{a_2}s_2[n-1]$  are sent to the  $k$ -th RS through  $h_{j,k}[n]$ , while  $\sqrt{a_1}s_1[n]$  and  $\sqrt{a_2}s_2[n]$  are sent to the  $k$ -th RS through  $h_{b,k}[n]$ . Let  $G_{k,1}[n] = a_1|h_{j,k}[n]|^2$ ,  $G_{k,2}[n] = a_2|h_{j,k}[n]|^2$ ,  $G_{k,3}[n] = a_1|h_{b,k}[n]|^2$ , and  $G_{k,4}[n] = a_2|h_{b,k}[n]|^2$ . Thus,  $G_{k,l}[n]$  ( $1 \leq l \leq 4$ ) denotes the effective channel gains of the  $l$ -th signals at the  $k$ -th RS in the  $n$ -th transmission phase. Let  $R'_l$  denote the target rate of the  $l$ -th signal. Then,  $R'_1 = R'_3 = R_1$  and  $R'_2 = R'_4 = R_2$ . The condition of successful decoding of the  $k$ -th RS such that  $k \notin \mathcal{D}[n-1]$  at the  $n$ -th transmission phase is given by the union of

$$\begin{aligned} \text{(C3): } & \log \left( 1 + \rho \sum_{l \in \mathcal{L}} G_{k,l}[n] \right) \geq \frac{N}{N-1} \sum_{l \in \mathcal{L}} R'_l, \\ & \forall \mathcal{L} \subset \{1, 2, 3, 4\}, \text{ and} \\ \text{(C4): } & \log \left( 1 + \frac{G_{k,1}[n] + G_{k,2}[n]}{G_{k,3}[n] + G_{k,4}[n] + 1/\rho} \right) \geq \frac{N(R_1 + R_2)}{N-1}. \end{aligned} \quad (5)$$

If either of the conditions in (5) is satisfied, then the joint decoding at the  $k$ -th RS succeeds. Thus, the left-hand side of (5) is expressed by the sum of the effective channel gains in  $\log(1 + \rho)$ , which is a well-known equation for analyzing a fading MAC capacity region in the literature, as Eq. (6.32) of [29]. The general MAC capacity region can be extended to an arbitrary number of users. Therefore, a pair of the desired signals and interference signals should be within the MAC capacity region for successful joint decoding as in [30].

### B. RS Selection

In this section, we explain how to select the RS for relaying the packet to two MSs at the  $n$ -th transmission phase. Obviously, the RSs that successfully decode the signal in the  $(n-1)$ -th transmission phase become candidates to be selected for relaying the packet in the  $n$ -th transmission phase. In this paper, we propose a *two-stage* RS selection algorithm. In the first stage, we define a set  $\mathcal{S}[n]$  based on the

following conditions:

$$\mathcal{S}[n] = \left\{ k \in \mathcal{D}[n-1] \left| \log \left( 1 + \frac{a_1 |g_{k,i}[n]|^2}{a_2 |g_{k,i}[n]|^2 + \frac{1}{\rho}} \right) \geq \frac{NR_1}{N-1}, \forall i = 1, 2 \right. \right\}, \quad (6)$$

where  $2 \leq n \leq N$ . Thus,  $s_1[n]$  from the RS in  $\mathcal{S}[n]$  will be successfully decoded at both MSs in the  $n$ -th transmission phase. In the second stage, the  $j$ -th RS in  $\mathcal{S}[n]$  is selected by the following criterion:

$$j = \arg \max_{k \in \mathcal{S}[n]} |g_{k,2}[n]|^2, \quad 2 \leq n \leq N. \quad (7)$$

The main difference between the proposed RS selection algorithm in this paper and [7] is that the RSs that successfully decoded both  $s_1[n-1]$  and  $s_2[n-1]$  are included in  $\mathcal{S}[n]$ , while the RSs that failed to decode  $s_2[n-1]$  can be included in  $\mathcal{S}[n]$  in the RS selection scheme in [7].

### C. Distributed Operations & Signaling Overhead

Under the CSIR assumption, the proposed RS selection algorithm can be implemented with a decentralized manner with a finite amount of feedback bits from the MSs. First of all, in the proposed RS selection algorithm, each RS except for the selected RS informs whether it successfully decoded the received signals from the BS by one bit to the MSs. In other words, each RS notifies whether it belongs to  $\mathcal{D}[n-1]$  or not to the MSs. In this step, the average signaling overhead is given by  $\mathbb{E}[|\mathcal{D}[n-1]|] = \sum_{t=0}^K \Pr\{|\mathcal{D}[n-1]|=t\} \cdot t$  bits. Then, the first MS checks if it can succeed to decode  $s_1[n-1]$  by dealing with  $s_2[n-1]$  as noise for all RSs included in  $\mathcal{D}[n-1]$ , and it sends the result to the second MS. In this step, the average signaling overhead is also given by  $\mathbb{E}[|\mathcal{D}[n-1]|]$  bits. Based on the feedback from the first MS and the RSs, the second MS can now check the condition in (7). Finally, the second MS selects the RS with criterion in (8) and feeds the index of the selected RS to RSs. In this step, the required signaling overhead is given by  $\log K$  bits. Thus, overall signaling overhead of the proposed algorithm at the  $n$ -th transmission phase is given by  $2 \cdot \sum_{t=0}^K \Pr\{|\mathcal{D}[n-1]|=t\} \cdot t + \log K$  bits. If all RSs, i.e.,  $K$  RSs notify whether it belongs to  $\mathcal{D}[n-1]$  or not, then  $K$  bits are always required. This is a basic and explicit operation. Meanwhile, in order to reduce the feedback overhead to the extent possible, we assume that a certain RS is acknowledged as not included in  $\mathcal{D}[n-1]$  if it does not notify its state, which can be regarded as an *implicit* feedback. That is why the signaling overhead is equal to  $\mathbb{E}[|\mathcal{D}[n-1]|]$  bits instead of  $K$  bits.

## IV. OUTAGE PROBABILITY ANALYSIS

In this section, we analyze the proposed VFD cooperative NOMA technique in terms of outage probability. In order to obtain the outage probability in the  $n$ -th phase, we need to consider the state of decoding set of the  $(n-1)$ -th transmission phase. Due to this Markovity, the outage probability in the

$n$ -th phase,  $\Pr\{\mathcal{O}_n\}$ , is given as

$$\begin{aligned} \Pr\{\mathcal{O}_n\} &= \sum_{t=0}^K \Pr\left\{\mathcal{O}_n \mid |\mathcal{S}[n]| = t\right\} \Pr\{|\mathcal{S}[n]| = t\} \\ &= \sum_{t=0}^K \Pr\left\{|g_{j,2}[n]|^2 < \frac{2^{\frac{NR_2}{N-1}} - 1}{a_2\rho} \mid |\mathcal{S}[n]| = t\right\} \cdot \Pr\{|\mathcal{S}[n]| = t\} \\ &= \sum_{t=0}^K \left(\Pr\left\{|g_{j,2}[n]|^2 < \frac{2^{\frac{NR_2}{N-1}} - 1}{a_2\rho}\right\}\right)^t \Pr\{|\mathcal{S}[n]| = t\}. \quad (8) \end{aligned}$$

Note that  $j$  denotes the index of the selected RS based on the selection criterion in (7). Unfortunately, the outage probability in (8) is intractable because the outage probability in the  $n$ -th transmission phase depends on  $|\mathcal{S}[n-1]|$ . That is, it is not straightforward to solve  $\Pr\{|\mathcal{S}[n]| = t\}$  directly since  $\Pr\{|\mathcal{S}[n]| = t\}$  depends on  $\Pr\{|\mathcal{S}[i]| = s\}$  in all the  $n-1$  previous phases, i.e.,  $\forall i = 1, \dots, n-1$ . Thus, we adopt a discrete Markov chain to obtain the closed-form solution of  $\Pr\{|\mathcal{S}[n]| = t\}$ , and then the outage probability can be obtained with steady state analysis, i.e.,  $\lim_{n \rightarrow \infty} \Pr\{\mathcal{O}_n\} = \Pr\{\mathcal{O}\}$ . For valid analysis based on the stationary distribution of a Markov chain, the Markov chain should be irreducible and aperiodic, in which either the states are all transient or all states are positive recurrent [31]. If all states of the Markov chain are positive recurrent, then the  $n$ -step transition probability to reach state  $j$ ,  $r_{ij}(n)$ , converges to a steady state probability  $\pi_j$  regardless of the initial state  $i$ . That is,

$$\pi = \lim_{n \rightarrow \infty} \mathbf{P}_i^n > 0 \quad (9)$$

where  $\mathbf{P}$  is a transition matrix of the Markov chain and  $\mathbf{P}_i^n$  is the  $i$ -th column of the matrix  $\mathbf{P}^n$ . Then,  $\pi$  has a unique stationary distribution. In this paper, we exploit the Markov chain whose states are related to the number of RS candidates for selection, and are significantly affected by channel conditions we consider. Moreover, the statistical property of wireless channel such as mean and variance should be unchanged. If it holds, a unique stationary distribution exists. In this paper, we assume that the statistical property of wireless channel is unchanged and thus we can apply this Markov model for state-dependent outage probability analysis. The following theorem states the outage probability of the proposed VFD cooperative NOMA technique in the steady state, when all nodes are equipped with a single antenna and there is no direct link between the BS and two MSs.

*Theorem 1:* Assuming  $K$  half-duplex RSs between the BS and two MSs, the outage probability of the VFD cooperative NOMA technique is given by

$$\Pr\{\mathcal{O}\} = \sum_{t=0}^K \left(1 - \exp\left(-\frac{2^{\frac{NR_2}{N-1}} - 1}{a_2\rho}\right)\right)^t \pi_t, \quad (10)$$

where  $\pi_t, \forall t \in \{0, \dots, K\}$  denotes a  $(K+1)$ -dimensional stationary distribution vector for the Markov chain. Thus,  $\pi \triangleq [\pi_0, \pi_1, \dots, \pi_K]$  and  $\sum_{i=0}^K \pi_i = 1$ .

*Proof:* Consider the Markov chain whose states represent the cardinality of  $\mathcal{S}$ . Then, the state transition matrix is defined as

$$\mathbf{P}_K = \begin{pmatrix} P_{0,0} & P_{0,1} & \dots & P_{0,K-1} & P_{0,K} \\ P_{1,0} & P_{1,1} & \dots & P_{1,K-1} & 0 \\ \vdots & \vdots & \ddots & \vdots & \vdots \\ P_{K-1,0} & P_{K-1,1} & \dots & P_{K-1,K-1} & 0 \\ P_{K,0} & P_{K,1} & \dots & P_{K,K-1} & 0 \end{pmatrix}, \quad (11)$$

where  $P_{i,j}$  denotes the transition probability from state  $i$  to  $j$ . More specifically,  $P_{i,j}$  means  $\Pr\{|\mathcal{S}[n-1]| = i \rightarrow |\mathcal{S}[n]| = j\}$  for the arbitrary transmission phase,  $n = 2, \dots, N$ . Note that the elements in the last column of  $\mathbf{P}_K$  are equal to zero except for the first element,  $P_{0,K}$ , because a selected RS cannot receive signals from the BS while transmitting signals due to half-duplex operation. Each element of  $\mathbf{P}_K$  is given by (12) on the bottom of this page, where  $p_1$  and  $p_2$  denote the probability that a RS is not included in  $\mathcal{S}$  in the absence of inter-relay interference signals and in the presence of inter-relay interference signals, respectively. Please note that the number of RSs that succeed decoding when  $i \neq 0$ ,  $j$  is determined by the sum of the number of the RSs that succeed decoding in the absence and presence of inter-RS interference,  $x$  and  $j-x$ , respectively among  $K-1$  RSs since the selected RS forwards the received signal at the same time.

We can easily confirm that the Markov chain reaches a steady state as in [28], which means that  $\pi\mathbf{P}_K = \pi$  holds. Solving  $\pi\mathbf{P}_K = \pi$  subject to  $\sum_{i=0}^K \pi_i = 1$ , we obtain the closed-form solution of  $\Pr\{|\mathcal{S}[n]| = t\}$  in the steady state, which indicates  $\Pr\{|\mathcal{S}[n]| = t\} = \pi_t$ . Recall that  $|h_{j,2}[n]|^2$  follows an exponential distribution with the unit mean. Then, we finally attain (10). ■

*Example 1:* When  $K = 3$ ,

$$\Pr\{\mathcal{O}\} = \sum_{t=0}^3 \left(1 - \exp\left(-\frac{2^{\frac{NR_2}{N-1}} - 1}{a_2\rho}\right)\right)^t \pi_t, \quad (13)$$

where

$$\pi_0 = \frac{\pi_2(P_{1,2} - P_{2,2} + 1) - P_{1,2}}{\mathcal{T}} \quad (14)$$

$$\pi_1 = 1 - (1 + P_{0,3})\pi_0 - \pi_2 \quad (15)$$

$$\pi_2 = \frac{\mathcal{T}(P_{1,1} - 1) - \mathcal{C}P_{1,2}}{\mathcal{C}(P_{2,2} - P_{1,2} - 1) + \mathcal{T}(P_{1,1} - P_{2,1} - 1)} \quad (16)$$

$$\pi_3 = 1 - \pi_0 - \pi_1 - \pi_2, \quad (17)$$

where  $\mathcal{T} = P_{0,2} + P_{0,3}P_{3,2} - P_{1,2} - P_{1,2}P_{0,3}$  and  $\mathcal{C} = 1 - P_{1,1} - P_{0,3}P_{1,1} + P_{0,1} + P_{0,3} + P_{0,3}P_{3,1}$ .

$$P_{i,j} = \begin{cases} \binom{K}{j} p_1^{K-j} (1-p_1)^j, & \text{if } i = 0 \\ \sum_{x=0}^{\min(i,j)} \binom{i-1}{x} p_1^{i-1-x} (1-p_1)^x \binom{K-i}{j-x} p_2^{K-i-j+x} (1-p_2)^{j-x}, & \text{if } i \neq 0 \end{cases} \quad (12)$$

*Proof:* Plugging  $K = 3$  in (10) and solving  $\pi \mathbf{P}_3 = \pi$ , we can easily obtain (13). ■

*Remark 1:* We can empirically confirm that  $\mathbf{P}_K^n \mathbf{P}_K \approx \mathbf{P}_K^n$  holds with small  $n (\leq 10)$  on average, which means the transition probability reaches a steady state after a relatively small number of transmission phases, compared with sufficiently large  $N$ . Thus, the analysis on the outage probability in (10) becomes justified.

## V. VFD COOPERATIVE NOMA WITH ADAPTIVE RESET

In this section, we propose a modified version of the VFD cooperative NOMA technique that adaptively resets the successive transmission at the BS. Recall that the BS sends a new super-imposed signal for two users in each transmission phase except for the last transmission phase, which is denoted as  $N$  in Section II. The RSs not belonging to  $\mathcal{S}$  suffer from interference from the selected RS and thus they are likely to fail in decoding the signal from the BS in a certain transmission phase. Then,  $|\mathcal{S}[n]|$  may become decreased. The basic idea of the adaptive reset is to allow the BS to stop transmitting the signal during a single transmission phase and then restart the proposed protocol when  $|\mathcal{S}[n]| \leq \kappa$  where  $\kappa$  is a positive integer.

### A. Outage Probability Analysis

Before the asymptotic analysis, we formulate the outage probability of the proposed virtual full-duplex cooperative NOMA with adaptive reset. When adaptive reset is adopted, the closed form of outage probability is changed from the different state transition matrix due to adaptive reset, which is defined by

$$\mathbf{P}_{\text{Adap}} = \begin{pmatrix} P_{0,0} & \dots & P_{0,K-1} & P_{0,K} \\ \vdots & \vdots & \vdots & \vdots \\ P_{0,0} & \dots & P_{0,K-1} & P_{0,K} \\ P_{K-\kappa,0} & \dots & P_{K-\kappa,K-1} & 0 \\ \vdots & \dots & \vdots & \vdots \\ P_{K,0} & \dots & P_{K,K-1} & 0 \end{pmatrix}. \quad (18)$$

Note that the first  $\kappa$  columns are the same since they are transition probabilities from the initial state due to refreshing and the elements except for the first  $\kappa + 1$   $P_{0,K}$ s in the last column are zero since a selected relay always forwards the received signals and thus the cardinality of  $\mathcal{S}$  cannot be  $K$  except for when adaptive reset is adopted. Adaptive reset alters the closed form of outage probability compared to (13) as follows:

*Corollary 1:* When  $K = 3$ ,

$$\Pr\{\mathcal{O}\} = \sum_{t=0}^3 \left( 1 - \exp\left(-\frac{2^{\frac{NR_2}{N-1}} - 1}{a_2 \rho}\right) \right)^t \pi_t, \quad (19)$$

where

$$\pi_0 = \frac{\{P_{2,0}P_{0,2} + P_{0,0}(1 - P_{2,2})\}\pi_2 + (P_{3,0}P_{0,2} - P_{3,2}P_{0,0})\pi_3}{P_{0,2}},$$

$$\pi_1 = 1 - \pi_0 - \pi_2 - \pi_3,$$

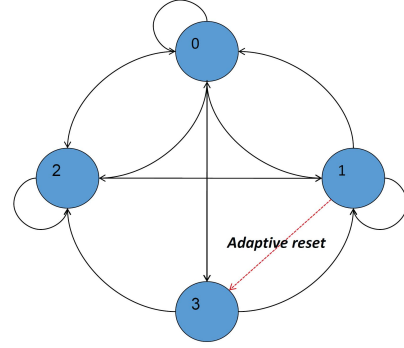


Fig. 2. An example of adaptive reset: The case for  $K = 3$  and  $\kappa = 1$ .

$$\pi_2 = \frac{P_{0,2} - P_{3,2}(P_{0,0} + P_{1,1} + P_{0,2})}{(1 + P_{0,3})(1 - P_{2,2}) - P_{0,2} + P_{3,2}(P_{0,0} + P_{1,1} + P_{0,2})},$$

$$\pi_3 = \frac{P_{0,3}(1 - \pi_2)}{1 + P_{0,3}}$$

where  $T = P_{0,2} + P_{0,3}P_{3,2} - P_{1,2} - P_{1,2}P_{0,3}$  and  $C = 1 - P_{1,1} - P_{0,3}P_{1,1} + P_{0,1} + P_{0,3} + P_{0,3}P_{3,1}$ .

*Proof:* Plugging  $K = 3$  in (10) and solving  $\pi \mathbf{P}_{\text{Adap}} = \pi$ , we can easily obtain (19). ■

### B. Diversity-Multiplexing Tradeoff (DMT)

Let  $\kappa$  be the cardinality of the decoding set which determines the time to restart the transmission protocol. For example,  $\kappa = 1$  means that the protocol restarts when  $|\mathcal{S}[n]| \leq 1$ , as shown in Fig. 2. The dotted red arrow from state 1 ( $\kappa$ ) to state 3 ( $K$ ) corresponds to adaptive reset, whereas the arrow does not exist if adaptive reset is not adopted. As a result, adaptive reset secures diversity gain even in the high multiplexing gain regime, which will be justified via asymptotic analysis later in this section.

In this context, we asymptotically analyze the proposed protocol with respect to  $\rho$ ,  $N$  and  $K$  based on outage probability analysis. Basically, we exploit DMT [32] as the main metric. For DMT analysis, note that multiplexing gain and diversity gain are defined, respectively, by  $r = \lim_{\rho \rightarrow \infty} \frac{\log R_i(\rho)}{\log \rho}$  and  $d = \lim_{\rho \rightarrow \infty} -\frac{\log P_{\text{out}}(\rho)}{\log \rho}$  where  $R_i(\rho)$  represents the transmission rate of MS  $i$ , and  $P_{\text{out}}$  denotes outage probability. Let us define  $f(\rho) \doteq \rho^v$  if  $\lim_{\rho \rightarrow \infty} \frac{\log(f(\rho))}{\log \rho} = v$ .  $a^+$  denotes  $\max(0, a)$  for any real value  $a$ , and  $\log(\cdot)$  denotes the base-2 logarithm. Focusing on DMT performance, substitute  $R_i$  with  $r_i \log \rho$  and define  $\pi_t \doteq \tilde{\pi}_t$  where  $\tilde{\pi}_t$ , an element of  $\tilde{\pi}$ , is the dominant scale of  $\pi_t$ . Then, the outage probability scales like

$$\Pr\{\mathcal{O}\} \doteq \sum_{t=0}^K \left( \frac{2^{\bar{r}_2 \log \rho}}{a_2 \rho} \right)^t \tilde{\pi}_t \doteq \sum_{t=0}^K \rho^{-t(1 - \bar{r}_2)} \cdot \tilde{\pi}_t, \quad (20)$$

where  $\bar{r}_i$  is effective multiplexing gain of MS  $i$  ( $\bar{r}_i = cr_i$ ), determined by the further asymptotic analysis shown later. In order to represent  $\tilde{\pi}_t$ , it is necessary to formulate the dominant scale of the outage probabilities conditioned on the decoding status of RS  $k$  in the previous phase. For the case when RS  $k$  succeeded decoding in the previous phase, the outage probability for RS  $k$  is the same as the case in the

absence of inter-relay interference due to SIC. Hence, we have

$$\begin{aligned}
p_o &= 1 - \Pr \left( |h_{b,k}[n]|^2 > \frac{2^{\bar{r}_2 \log \rho}}{\rho} \right) \\
&\quad \times \Pr \left( |h_{b,k}[n]|^2 > \frac{2^{\bar{r}_1 \log \rho} - 1}{\{a_1 - (2^{\bar{r}_1 \log \rho})a_2\}\rho} \right) \\
&\quad \times \Pr \left( |g_{k,1}[n]|^2 > \frac{2^{\bar{r}_1 \log \rho} - 1}{\{a_1 - (2^{\bar{r}_1 \log \rho})a_2\}\rho} \right) \\
&\quad \times \Pr \left( |g_{k,2}[n]|^2 > \frac{2^{\bar{r}_1 \log \rho} - 1}{\{a_1 - (2^{\bar{r}_1 \log \rho})a_2\}\rho} \right) \\
&= 1 - \exp \left\{ -\frac{2^{\bar{r}_2 \log \rho}}{\rho} - 3 \frac{2^{\bar{r}_1 \log \rho} - 1}{\{a_1 - (2^{\bar{r}_1 \log \rho})a_2\}\rho} \right\} \\
&\doteq \frac{2^{\bar{r}_2 \log \rho}}{\rho} + 3 \frac{2^{\bar{r}_1 \log \rho}}{\{a_1 - (2^{\bar{r}_1 \log \rho})a_2\}\rho} \\
&\doteq \rho^{\bar{r}_2 - 1} + 3 \frac{\rho^{\bar{r}_1}}{\rho - \rho^{\bar{r}_1 + 1}} \doteq \rho^{-(1 - \bar{r}_2)}, \tag{21}
\end{aligned}$$

since  $\frac{\rho^{\bar{r}_1}}{\rho - \rho^{\bar{r}_1 + 1}}$  goes to zero when  $\rho$  is sufficiently large. Meanwhile, assuming  $P_{\text{MAC}}$  denotes the probability that (5) holds,

$$\begin{aligned}
p_{o_{\text{int}}} &= 1 - P_{\text{MAC}} \Pr \left( |g_{k,1}[n]|^2 > \frac{2^{\bar{r}_1 \log \rho} - 1}{\{a_1 - (2^{\bar{r}_1 \log \rho})a_2\}\rho} \right) \\
&\quad \times \Pr \left( |g_{k,2}[n]|^2 > \frac{2^{\bar{r}_1 \log \rho} - 1}{\{a_1 - (2^{\bar{r}_1 \log \rho})a_2\}\rho} \right) \\
&\doteq \rho^{-(1 - \bar{r}_i)} + \rho^{-2(1 - 2\bar{r}_i)} + \rho^{-(1 - \sum_l \bar{r}_l)} + \rho^{-2(1 - \bar{r}_1 - 2\bar{r}_2)} \\
&\quad + \rho^{-2(1 - 2\bar{r}_1 - \bar{r}_2)} + \rho^{-2(1 - 2\sum_l \bar{r}_l)} + 2 \frac{\rho^{\bar{r}_1}}{\rho - \rho^{\bar{r}_1 + 1}} \\
&\doteq \rho^{-\min(1 - \bar{r}_i, 2(1 - 2\bar{r}_i), 1 - \sum_l \bar{r}_l, 2(1 - \bar{r}_1 - 2\bar{r}_2), 2(1 - 2\bar{r}_1 - \bar{r}_2), 2(1 - 2\sum_l \bar{r}_l))} \tag{22}
\end{aligned}$$

for all  $i = 1, 2$  where  $\sum_l \bar{r}_l = \bar{r}_1 + \bar{r}_2$ .

However, it is intractable and complicated to attain the dominant scale of the stationary probability of the Markov chain,  $\tilde{\pi}_t$ . Hence, as assumed in [33] and [34] in order to effectively characterize DMT for each individual multiplexing gain, we deal with symmetric multiplexing gain case ( $r_1 = r_2 = r$ ). The symmetric multiplexing case is acceptable since the multiplexing gain of each user can be the same though the achievable rate of each user is different for NOMA, *i.e.*, we can say  $r_1 = r_2 = r$  if  $R_1 > R_2$  and  $R_1 \doteq R_2 \doteq \rho^r$ . Since  $r_1 = r_2 = r$  implies  $\bar{r}_1 = \bar{r}_2 = \bar{r}$ , under the assumption of symmetric multiplexing gain, (21) and (22) are reduced to

$$p_o \doteq \rho^{-\min(1 - \bar{r})}, \quad p_{o_{\text{int}}} \doteq \rho^{-\min(1 - 2\bar{r}, 2(1 - 4\bar{r}))}, \tag{23}$$

respectively. Based on (23), we have the closed form of DMT of the proposed protocol.

*Theorem 2:* Assuming  $K$  half-duplex RSs between the BS and two MSs, the DMT of the virtual full-duplex cooperative NOMA technique with adaptive reset for  $\kappa$  is given by (24) on the bottom of this page.

*Proof:* Plugging (23) into (18), we will obtain  $\tilde{\pi}$  which  $\mathbf{P}_{\text{Adap}} \doteq \mathbf{P}_{\text{Adap}}^n \mathbf{P}_{\text{Adap}}$  holds. In order to find the dominant scale of converged transition probability, three mainly different multiplexing gain regions should be classified since  $p_{o_{\text{int}}} \doteq \rho^{-(1 - 2\bar{r})}$  for  $0 \leq \bar{r} \leq \frac{1}{6}$ ,  $p_{o_{\text{int}}} \doteq \rho^{-2(1 - 4\bar{r})}$  for  $\frac{1}{6} \leq \bar{r} \leq \frac{1}{4}$ , and  $p_{o_{\text{int}}} \doteq \rho^0$  for  $\frac{1}{4} \leq \bar{r}$ .

For  $0 \leq \bar{r} \leq \frac{1}{6}$ , by matrix multiplications, we can obtain

$$\mathbf{P}_{\text{Adap},0}^5 = \dots = \mathbf{P}_{\text{Adap},K}^5 \doteq \left[ \rho^{-((K-1) - K\bar{r})}, \rho^{-((K-2) - (K-1)\bar{r})}, \rho^{-((K-3) - (K-2)\bar{r})}, \dots, \rho^0, \rho^{-((K-1) - K\bar{r})} \right], \tag{25}$$

where  $\mathbf{P}_{\text{Adap},k}$  is the  $k$ -th row of  $\mathbf{P}_{\text{Adap}}$ . Since  $\mathbf{P}_{\text{Adap}}^5 \doteq \dots \doteq \mathbf{P}_{\text{Adap}}^n$ ,  $\tilde{\pi} \doteq \mathbf{P}_{\text{Adap},k}^5 \doteq \dots \doteq \mathbf{P}_{\text{Adap},k}^n$ .

For  $\frac{1}{6} \leq \bar{r} \leq \frac{1}{4}$ , once a multiplication of  $\mathbf{P}_{\text{Adap}}$  is performed, the dominant scale of  $\mathbf{P}_{\text{Adap}}$  is divided into two multiplexing gain regimes. The divided multiplexing gain regimes are totally up to  $K - 1 - \kappa$ , and the dominant scale of each element varies according to the regime. For example, when  $K = 4$  and  $\kappa = 1$ , two different dominant scales of  $\mathbf{P}_{\text{Adap}}$  can be obtained, then the stationary distribution is finally formulated with the minimum of those dominant scales. It is similar that the dominant scale of every row of  $\mathbf{P}_{\text{Adap}}$  becomes equivalent after not many number of multiplications of  $\mathbf{P}_{\text{Adap}}$ . For  $1/4 \leq \bar{r}$ , we can also obtain the dominant scale of stationary distribution in a similar way for the case of  $0 \leq \bar{r} \leq \frac{1}{6}$ .

Consequently, we have

$$\tilde{\pi} \doteq \left[ \rho^{-((K-1) - K\bar{r})}, \rho^{-((K-2) - (K-1)\bar{r})}, \rho^{-((K-3) - (K-2)\bar{r})}, \dots, \rho^0, \rho^{-((K-1) - K\bar{r})} \right] \text{ for } 0 \leq \bar{r} \leq 1/6 \tag{26}$$

$\tilde{\pi} \doteq \min_{i=1, \dots, K-1-\kappa} \tilde{\pi}^{(i)}$ , for  $1/6 \leq \bar{r} \leq 1/4$ , where

$$\begin{aligned}
\tilde{\pi}^{(i)} &= \left[ \rho^{-\{(K-i-1)(1-\bar{r}) + (i^2+i)(1-4\bar{r})\}}, \right. \\
&\quad \left. \rho^{-\{(K-i-2)(1-\bar{r}) + (i^2+i)(1-4\bar{r})\}}, \dots, \rho^{-2(1-4\bar{r})}, \rho^0, \right. \\
&\quad \left. \rho^{-\{(K-i-1)(1-\bar{r}) + (i^2+i)(1-4\bar{r})\}} \right], \tag{27}
\end{aligned}$$

$$\tilde{\pi} \doteq \left[ \rho^{-\kappa(1-\bar{r})}, \dots, \rho^{-(1-\bar{r})}, \rho^0, \dots, \rho^0 \right] \text{ for } 1/4 \leq \bar{r}. \tag{28}$$

Now, we identify effective multiplexing gain,  $\bar{r}$  for each multiplexing gain regime. For  $0 \leq \bar{r} \leq \frac{1}{4}$ , since  $\rho^0$  is only in the  $K$ -th element of  $\tilde{\pi}$ ,

$$\lim_{\rho \rightarrow \infty} \tilde{\pi} \approx [0 \ 0 \ \dots \ 0 \ 1 \ 0]. \tag{29}$$

$$d(r, K, \kappa) = \begin{cases} K - 1 - Kr, & \text{if } 0 \leq r \leq \frac{1}{6} \\ \min_{i=1, \dots, K-1-\kappa} \{(K-1-i)(1-r) + (i^2+i)(1-4r)\}, & \text{if } \frac{1}{6} \leq r \leq \frac{1}{4} \\ \kappa \left(1 - \frac{K-\kappa+1}{K-\kappa} r\right)^+, & \text{if } \frac{1}{4} \leq r \leq 1 \end{cases} \tag{24}$$

That is,  $\lim_{\rho \rightarrow \infty} \pi_{K-1} \approx 1$  and  $\lim_{\rho \rightarrow \infty} \pi_t \approx 0, \forall t \neq K-1$  where  $\pi_t$  is the steady state probability of state  $t$  corresponding to  $(t+1)$ -th element of  $\boldsymbol{\pi}$ . It implies that no refreshing is needed in asymptotic region, thus  $\bar{r} = r$  for  $0 \leq \bar{r} \leq \frac{1}{4}$ . Note that two limits about  $n$  and  $\rho$  are independent so that the order of limits is irrelevant to the DMT results throughout this paper.

Meanwhile, for  $\frac{1}{4} \leq \bar{r}$ , since  $\rho^0$  appears in the last  $K-\kappa+1$  elements,

$$\lim_{\rho \rightarrow \infty} \tilde{\boldsymbol{\pi}} \approx [0 \ 0 \ \cdots \ c_\kappa \ \cdots \ c_{K-1} \ c_K] \quad (30)$$

and it is easily shown that all the coefficients of  $\rho^0$  are the same. Therefore,  $c_\kappa = \cdots = c_K = \frac{1}{K-\kappa+1}$  and  $\bar{r} = \frac{K-\kappa+1}{K-\kappa}r$  for  $\frac{1}{4} \leq \bar{r}$  because adaptive reset occurs when  $|S[n]| \leq \kappa$ .

Replacing  $\tilde{\pi}_t$  in (20) by the elements of  $\tilde{\boldsymbol{\pi}}$ , we can obtain (24). ■

*Corollary 2:* The proposed protocol approximately achieves the upper bound of DMT For  $0 \leq r \leq \frac{1}{4}$  as  $K$  increases given the optimal value of  $\kappa = K-2$ .

*Proof:* For  $0 \leq r \leq \frac{1}{4}$ , since  $\lim_{\rho \rightarrow \infty} \pi_{K-1} \approx 1, \kappa = K-2$  maximizes  $d(r, K, \kappa)$ . Then, we have

$$\begin{aligned} & \lim_{K \rightarrow \infty} d(r, K, \kappa)|_{\kappa=K-2} \\ &= \lim_{K \rightarrow \infty} \min \{(K-1) - Kr, K - (K+6)r\} \\ &\simeq \min \{(K-1)(1-r), K(1-r)\} \\ &= (K-1)(1-r) = d_u(r, K). \end{aligned} \quad (31)$$

Note that the upper bound reflects that a selected relay cannot always contribute to diversity gain. ■

## VI. NUMERICAL RESULTS

In this section, we evaluate the performance of the proposed technique and compare it with the conventional techniques including [7] in terms of outage probability. ‘Proposed’, ‘Two-stage RS’, and ‘Successive’ stand for the proposed technique in this paper, the two-stage RS selection technique proposed in [7], and the successive transmission based on the RS selection algorithm that always deals with the inter-RS interference as noise, respectively.  $R_1$  and  $R_2$  are set to 0.5 bits/s/Hz and 2 bits/s/Hz, respectively. We assume that  $N = 20$  for the proposed technique and the ‘Successive’ relaying technique.

Before we begin to show the numerical results in earnest, we verify the accuracy of the snapshot approach using a Markov chain when the number of phases is not extremely large as shown in Fig. 3. The outage probability from Eq. (13) matches well with the outage probability by Monte-Carlo simulation. That is, the simulation results validate the theoretical analysis using the steady state probability of the decoding set cardinality. Therefore, an arbitrary number of transmission phases can be incorporated in the outage probability analysis using a Markov chain.

Fig. 4 and 5 show the outage probability of the proposed technique for varying SNRs when  $K = 5$  and  $K = 10$ , respectively.

When  $K = 5$  and  $a_1 = 0.75$ , we have compared the performances of NOMA and OMA techniques in terms of outage probability as shown in Fig. 4, where ‘Two-hop OMA’

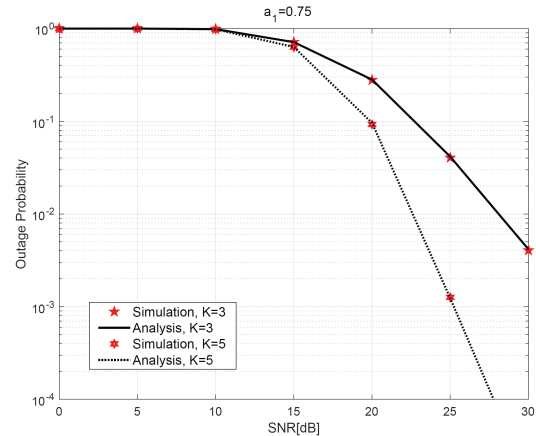


Fig. 3. Comparison simulation of outage probability of the proposed protocol with analysis when  $K = 3, \kappa = 0, R_1 = 0.5$  bits/s/Hz and  $R_2 = 2$  bits/s/Hz for 20 phases.

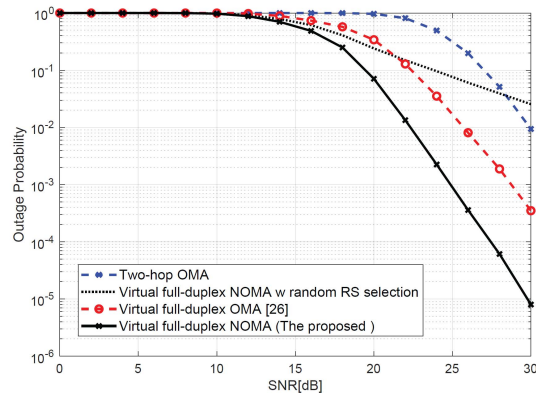


Fig. 4. Outage probability comparison between the OMA and NOMA based schemes when  $K = 5$  ( $R_1 = 0.5$  bits/s/Hz and  $R_2 = 2$  bits/s/Hz).

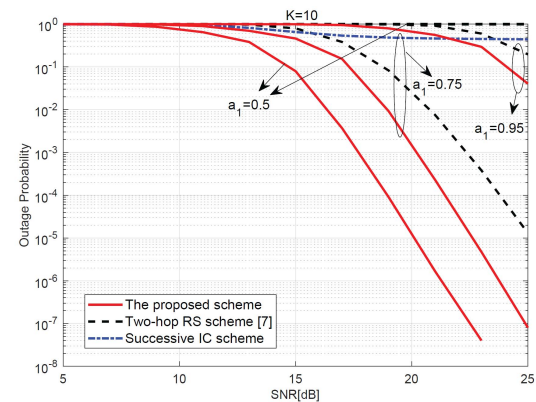


Fig. 5. Outage probability for varying SNR values when  $K = 10$  ( $R_1 = 0.5$  bits/s/Hz and  $R_2 = 2$  bits/s/Hz).

stands for the orthogonal multiple access (OMA) based on the opportunistic relaying technique with half-duplex RSs. Thus, each desired signal for two MSs is transmitted during four transmission phases. In addition, ‘Virtual full-duplex OMA’ stands for the opportunistic successive relaying protocol based on the OMA where each desired signal for two MSs is

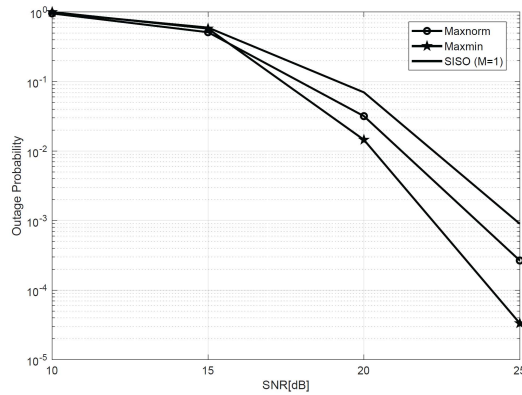


Fig. 6. Outage probability of the proposed technique according to beamforming technique when the number of antennas at the BS is equal to 5 ( $M = 5$ ).

transmitted during three transmission phases, where the signal for MS2, for instance, is transmitted to RSs from the BS when the signal for MS1 is forwarded by the selected RS at the same time.

In Fig. 4, ‘Virtual full-duplex NOMA’ and ‘Virtual full-duplex NOMA w random RS selection’ denote the proposed technique and the proposed NOMA technique based on random RS selection, respectively. Thus, ‘Virtual full-duplex NOMA w random RS selection’ is the same as the proposed scheme except for the method of RS selection. The OMA techniques are surpassed by the proposed technique in terms of outage probability even though the OMA signals are transmitted by the successive relaying manner.

If we adopt the random RS selection for the virtual full-duplex NOMA technique, then the outage probability becomes worse than that of the proposed technique since the selection diversity gain cannot be fully exploited. However, even the random RS selection based virtual full-duplex NOMA technique outperforms the two OMA based schemes when SNR is lower than 21 dB. When SNR is lower than 15 dB, the two schemes yield similar performance since both schemes do not work well due to severe noise effects. This SNR regime cannot be further increased theoretically because we assume not only the fixed target data rate without CSIT but also the outage probability is computed based on Shannon limit assuming the ideal channel coding.

When  $K = 10$  as shown in Fig. 5, the proposed technique outperforms both the two-stage RS technique [7] and the successive relaying technique especially for various values of  $a_1$ . The *optimal*  $a_1$ , resulting in the lowest outage probability, is different for the proposed technique and the two-stage RS technique. For example, the outage performance of the proposed technique when  $a_1 = 0.5$  is better than the case when  $a_1 = 0.75$  and  $a_1 = 0.95$ . However, the outage performance of the two-stage RS selection algorithm with  $a_1 = 0.75$  is better than the case when  $a_1 = 0.5$  and  $a_1 = 0.95$ .

We show the outage probability of the proposed technique according to several inter-RS distances as shown in Fig. 7. We change the variance of inter-RS channels to take into account the effect of inter-RS distances, while retaining the assumption of the same BS-to-RSs and RSs-to-MSs distance.

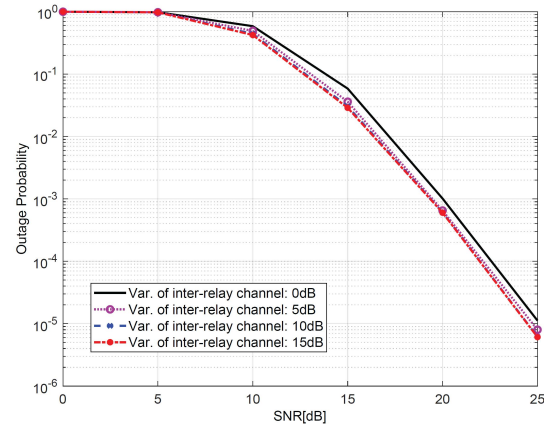


Fig. 7. Comparison of outage probability according to the inter-relay distances when  $K = 5$  and  $a_1 = 0.75$ .

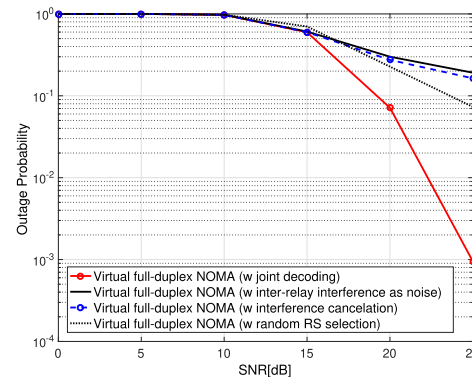


Fig. 8. Comparison of outage probability according to the strategies how to select RS when  $K = 5$  and  $a_1 = 0.75$ .

This geometry can be understood that RSs are located on the circle that is the bottom of two equivalent cones where the two cones are faced on the bottom of each other. We assume RSs are randomly deployed. As the variance of the inter-relay wireless channels increases, i.e., the RSs are located more closely to each other, the outage probability performance becomes even better as shown in Fig. 7. This is because the performance of joint decoding becomes improved as the inter-relay distance decreases, whereas the performance of the successive interference cancellation technique is affected by not the distance but whether the RS succeeds decoding in the previous phase. Furthermore, the worst case scenario in terms of outage probability is when the variance of the inter-relay channel is equal to 0 dB because the relay stations are deployed between the base stations and mobile stations in general, which is the system model that we originally considered in the previous manuscript. Thus, we can interpret the presented outage probability of the proposed scheme in the case where the variance of inter-RS channel is 0 dB as the upper bound of the cases when the RSs are more crowded, i.e., the variance of inter-RS channels is greater than 0 dB.

In Fig. 8, we show the outage probability of the proposed scheme based on several RS selection criterion, summarized in TABLE I in the next page. ‘Virtual full-duplex NOMA

TABLE I  
THE RS SELECTION SCHEMES IN THE SINGLE ANTENNA CASE FOR  $2 \leq n \leq N$

Scheme name	RS selection criterion
Virtual full-duplex NOMA (w joint decoding)	(7)
Virtual full-duplex NOMA (w inter-relay interference as noise)	(7) for $\mathcal{D}[n] = \left\{ k \mid \log \left( 1 + \frac{G_{k,1}[n] + G_{k,2}[n]}{G_{k,3}[n] + G_{k,4}[n] + 1/\rho} \right) \geq \frac{N(R_1 + R_2)}{N-1} \right\}$
Virtual full-duplex NOMA (w interference cancellation)	(7) for $\mathcal{D}[n] = \left\{ k \mid \log \left( 1 + \frac{G_{k,1}[n] + G_{k,2}[n]}{G_{k,3}[n] + G_{k,4}[n] + 1/\rho} \right) \geq \frac{N(R_1 + R_2)}{N-1} \right\}$ if $\log \left( 1 + \frac{G_{k,3}[n] + G_{k,4}[n]}{G_{k,1}[n] + G_{k,2}[n] + 1/\rho} \right) < \frac{N(R_1 + R_2)}{N-1}$ , $\mathcal{D}[n] = \left\{ k \mid (3) \text{ and } (4) \right\}$ if $\log \left( 1 + \frac{G_{k,3}[n] + G_{k,4}[n]}{G_{k,1}[n] + G_{k,2}[n] + 1/\rho} \right) \geq \frac{N(R_1 + R_2)}{N-1}$
Virtual full-duplex NOMA (w random RS selection)	$j = \text{random}(k)_{k \in \mathcal{S}[n]}$ .

(w joint decoding)” indicates the propose technique in this manuscript. In “Virtual full-duplex NOMA (w inter-relay interference as noise)”, the RSs decode the received signals from the BS by treating the inter-RS interference as noise in every phase. Meanwhile, the RSs for “Virtual full-duplex NOMA (w interference cancellation)” try to decode inter-RS interference beforehand, and then they dynamically determine how to decode the desired signals. If the RSs succeed the decoding of inter-RS interference, then they remove the interference and perform interference-free decoding of the signals from the BS. Otherwise, the RSs decode the desired signals by treating the inter-RS interference as noise. Outage probability of those schemes except for our proposed technique becomes saturated as SNR increases due to residual inter-RS interference. The slight performance gap between the two referential schemes comes from the fact that “Virtual full-duplex NOMA (w interference cancellation)” has a chance to decode the desired signal in the absence of the inter-RS interference. We have also considered the random RS selection criterion as shown in “Virtual full-duplex NOMA (w random RS selection)” in Fig. B and we confirm that its performance in terms of outage probability is equivalent to the  $K = 1$  case.

To rigorously analyze the multi-antenna scenarios, we should find the optimal beamformer for the proposed scheme. Let the number of antennas at the BS be  $M$  and the channel vector from the BS to RS  $k$  in the  $n$ -th phase be  $\mathbf{h}_{b,k}[n] \in \mathbb{C}^{M \times 1}$ .  $\mathbf{H}[n] \triangleq [\mathbf{h}_{b,1}[n] \ \mathbf{h}_{b,2}[n] \ \cdots \ \mathbf{h}_{b,K}[n]]^T \in \mathbb{C}^{K \times M}$  denotes the composite channel matrix where  $(\cdot)^T$  is the transpose of a matrix or a vector. From now we omit the index of phase without loss of the generality for convenience. At the BS, we consider two beamforming techniques according to the following criteria:

- Max-norm beamformer:

$$\mathbf{w}_{\text{norm}} = \arg \max_{\mathbf{w}} \|\mathbf{H}\mathbf{w}\|^2 \quad \text{subject to } \|\mathbf{w}_{\text{norm}}\|^2 = 1 \quad (32)$$

- Max-min beamformer:

$$\mathbf{w}_{\text{maxmin}} = \arg \max_{\mathbf{w}} \min_k |\mathbf{h}_{b,k}\mathbf{w}|^2 \quad \text{subject to } \|\mathbf{w}_{\text{maxmin}}\|^2 = 1 \quad (33)$$

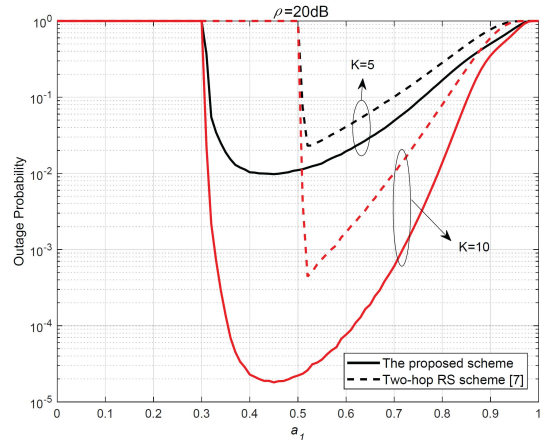


Fig. 9. Outage probability according to  $a_1$  when  $\rho = 20$  dB ( $R_1 = 0.5$  bits/s/Hz and  $R_2 = 2$  bits/s/Hz).

Fig. 6 illustrates the outage probability of the proposed technique with the previously-mentioned beamformers when the number of antennas at BS is equal to 5. Maxnorm, Maxmin, and SISO in Fig. A stand for the proposed scheme with the max-norm beamformer, the max-min beamformer, and a single antenna case at the BS ( $M = 1$ ), respectively. As seen in Fig. A, the max-min beamformer outperforms the max-norm beamformer in terms of outage probability. As we noted before, to retain the enough candidates for RS selection is essential to achieve better outage probability performance in the proposed technique, and thus we can say that the max-min beamformer is the most beneficial among various beamforming techniques.

Fig. 9 compares the outage probabilities of the proposed technique and the two-stage RS selection technique [7] according to  $a_1$  when  $\rho = 20$  dB. For  $K = 5$ , the optimal  $a_1$  of the proposed protocol that minimizes the outage probability is equal to 0.45 and the resultant outage probability is equal to  $9.77 \times 10^{-3}$ , while the optimal  $a_1$  of the two-stage RS selection technique [7] that minimizes the outage probability is equal to 0.52 and the resultant outage probability is equal to  $2.31 \times 10^{-2}$ . For  $K = 10$ , the optimal  $a_1$  of the proposed protocol that minimizes the outage probability is equal

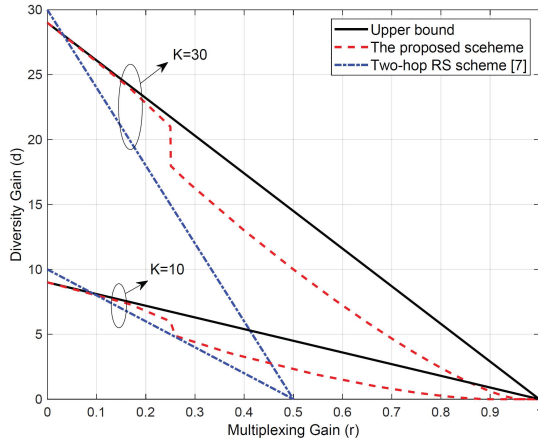


Fig. 10. DMT when  $K = 10, 30$ .

to 0.45 and the resultant outage probability is equal to  $1.80 \times 10^{-5}$ , while the optimal  $a_1$  of the two-stage RS selection technique [7] that minimizes the outage probability is equal to 0.52 and the resultant outage probability is equal to  $4.43 \times 10^{-4}$ . The optimal  $a_1$  in both the proposed technique and the two-stage RS selection technique [7] remains unchanged regardless of  $K$ .

In view of the outage probability, the superiority of the proposed protocol over the referential scheme becomes more significant as  $K$  increases because a selected relay is excluded from the decoding set, thus diversity gain becomes  $K - 1$ . However, when  $K = 5$ , the effect of the reduced diversity gain due to the selected relay can be marginal compared to the entire number of relays. As a result, the proposed protocol outperforms the two-stage relay selection scheme in terms of outage probability regardless of  $a_1$  for at least  $K \geq 5$ .

It is worthwhile noting that the regime where outage probability becomes 1 if  $a_1 \leq (2^{\frac{N}{N-1}R_1} - 1)a_2$ , the outage probability becomes 1 as confirmed in [2]. For the two-stage relay selection scheme, since  $2^{\frac{N}{N-1}R_1} - 1 = 1$ , the outage probability becomes 1 if  $a_1$  is less than or equal to  $a_2$ . Since the condition that outage always happens hinges on spectral efficiency, the schemes based on successive transmissions can have a wider regime of  $a_1$  where the outage probability is not equal to 1. Meanwhile, for the proposed protocol, when  $N = 20$  and  $R_1 = 0.5$  as set for the simulations,  $a_1$  should be greater than about 0.3057 to avoid to outage probability of 1, obtained by solving  $a_1 > (2^{\frac{10}{19}} - 1)(1 - a_1)$ . In conventional NOMA, it is commonly understood that more power portion is assigned to the high-priority user ( $a_1 \leq a_2$  if  $R_1 \leq R_2$ ). However, we find the inherent feature that less power portion of a high-priority user can be necessary. Basically, the counter-intuitive observation comes from the essence of the proposed protocol that the previous superimposed signal becomes the present interference. As such, power allocation strategies taking into account inter-relay interference can be varied compared to the concept of the conventional NOMA.

Fig. 10 compares DMT of the proposed protocol and two-stage relay selection when  $K = 10$  and 30. The upper bounds are plotted based on (31). In both  $K = 10$  and

30 cases, the proposed protocol outperforms the two-stage relay selection in terms of DMT except for the low multiplexing gain regime because there is an inherent difference of diversity gain between the proposed protocol and two-stage relay selection, in which a single relay in the proposed protocol is always excluded to be selected for VFD operation. For  $0 \leq r \leq \frac{1}{4}$ , DMT of the proposed protocol approaches the upper bound, and it validates *Corollary 2*.

## VII. CONCLUSION

We considered a single cell NOMA downlink network that consists of a BS, two MSs, and  $K$  half-duplex DF RSs. In this paper, we propose a novel virtual full-duplex cooperative NOMA framework in which the BS sends the superposed signals for two MSs in each transmission phase, while a selected RS sends the signals to two MSs at the same time. A two-stage RS selection algorithm is proposed and the outage probability of the proposed technique is mathematically derived. The allocated powers to two MSs need to be carefully adjusted for better performance in the proposed framework. The simulation results validate the performance of the proposed RS selection algorithm. In particular, the proposed virtual full-duplex cooperative NOMA framework outperforms the conventional half-duplex cooperative NOMA, which yields the best performance in terms of outage probability as well as DMT.

## REFERENCES

- [1] Y. Saito, Y. Kishiyama, A. Benjebbour, T. Nakamura, A. Li, and K. Higuchi, "Non-orthogonal multiple access (NOMA) for cellular future radio access," in *Proc. IEEE Veh. Technol. Conf.*, Dresden, Germany, Jun. 2013, pp. 1–5.
- [2] W. Shin, M. Vaezi, B. Lee, D. J. Love, J. Lee, and H. V. Poor, "Non-orthogonal multiple access in multi-cell networks: Theory, performance, and practical challenges," *IEEE Commun. Mag.*, vol. 55, no. 10, pp. 176–183, Oct. 2017.
- [3] Z. Ding, Z. Yang, P. Fan, and H. V. Poor, "On the performance of nonorthogonal multiple access in 5G systems with randomly deployed users," *IEEE Signal Process. Lett.*, vol. 21, no. 12, pp. 1501–1505, Dec. 2014.
- [4] S. Timotheou and I. Krikidis, "Fairness for non-orthogonal multiple access in 5G systems," *IEEE Signal Process. Lett.*, vol. 22, no. 10, pp. 1647–1651, Oct. 2015.
- [5] Z. Ding, L. Dai, and H. V. Poor, "MIMO-NOMA design for small packet transmission in the Internet of Things," *IEEE Access*, vol. 4, pp. 1393–1405, 2016.
- [6] J.-B. Kim and I.-H. Lee, "Non-orthogonal multiple access in coordinated direct and relay transmission," *IEEE Commun. Lett.*, vol. 19, no. 11, pp. 2037–2040, Nov. 2015.
- [7] Z. Ding, H. Dai, and H. V. Poor, "Relay selection for cooperative NOMA," *IEEE Wireless Commun. Lett.*, vol. 5, no. 4, pp. 416–419, Aug. 2016.
- [8] X. Yue, Y. Liu, S. Kang, and A. Nallanathan, "Performance analysis of NOMA with fixed gain relaying over Nakagami- $m$  fading channels," *IEEE Access*, vol. 5, pp. 5445–5454, 2017.
- [9] H. Sun, Q. Wang, R. Q. Hu, and Y. Qian, "Outage probability study in a NOMA relay system," in *Proc. IEEE Wireless Commun. Netw. Conf.*, San Francisco, CA, USA, Mar. 2017, pp. 1–6.
- [10] M. F. Kader, M. B. Shahab, and S. Y. Shin, "Exploiting non-orthogonal multiple access in cooperative relay sharing," *IEEE Commun. Lett.*, vol. 21, no. 5, pp. 1159–1162, May 2017.
- [11] X. Liang, Y. Wu, D. W. K. Ng, Y. Zuo, S. Jin, and H. Zhu, "Outage performance for cooperative NOMA transmission with an AF relay," *IEEE Commun. Lett.*, vol. 21, no. 11, pp. 2428–2431, Nov. 2017.
- [12] W. Shin, H. Yang, M. Vaezi, J. Lee, and H. V. Poor, "Relay-aided NOMA in uplink cellular networks," *IEEE Signal Process. Lett.*, vol. 24, no. 12, pp. 1842–1846, Dec. 2017.

- [13] R. Jiao, L. Dai, J. Zhang, R. MacKenzie, and M. Hao, "On the performance of NOMA-based cooperative relaying systems over Rician fading channels," *IEEE Trans. Veh. Technol.*, vol. 66, no. 12, pp. 11409–11413, Jul. 2017.
- [14] J. So and Y. Sung, "Improving non-orthogonal multiple access by forming relaying broadcast channels," *IEEE Commun. Lett.*, vol. 20, no. 9, pp. 1816–1819, Sep. 2016.
- [15] C. Zhong and Z. Zhang, "Non-orthogonal multiple access with cooperative full-duplex relaying," *IEEE Commun. Lett.*, vol. 20, no. 12, pp. 2478–2481, Dec. 2016.
- [16] Z. Zhang, Z. Ma, M. Xiao, Z. Ding, and P. Fan, "Full-duplex device-to-device-aided cooperative nonorthogonal multiple access," *IEEE Trans. Veh. Technol.*, vol. 66, no. 5, pp. 4467–4471, May 2017.
- [17] L. Zhang, J. Liu, M. Xiao, G. Wu, Y.-C. Liang, and S. Li, "Performance analysis and optimization in downlink NOMA systems with cooperative full-duplex relaying," *IEEE J. Sel. Areas Commun.*, vol. 35, no. 10, pp. 2398–2412, Oct. 2017.
- [18] B. Zheng, X. Wang, M. Wen, and F. Chen, "NOMA-based multi-pair two-way relay networks with rate splitting and group decoding," *IEEE J. Sel. Areas Commun.*, vol. 35, no. 10, pp. 2328–2341, Oct. 2017.
- [19] M. Mohammadi, B. K. Chalise, A. Hakimi, Z. Mobini, H. A. Suraweera, and Z. Ding, "Beamforming design and power allocation for full-duplex non-orthogonal multiple access cognitive relaying," *IEEE Trans. Commun.*, vol. 66, no. 12, pp. 5952–5965, Dec. 2018.
- [20] Z. Mobini, M. Mohammadi, H. A. Suraweera, and Z. Ding, "Full-duplex multi-antenna relay assisted cooperative non-orthogonal multiple access," in *Proc. IEEE GLOBECOM*, Singapore, Dec. 2017, pp. 1–7.
- [21] Y. Alsaba, C. Y. Leow, and S. K. A. Rahim, "Full-duplex cooperative non-orthogonal multiple access with beamforming and energy harvesting," *IEEE Access*, vol. 6, pp. 19726–19738, Apr. 2018.
- [22] L. Lei, E. Lagunas, S. Chatzinotas, and B. Ottersten, "NOMA aided interference management for full-duplex self-backhauling hetnets," *IEEE Commun. Lett.*, vol. 22, no. 8, pp. 1696–1699, Aug. 2018.
- [23] M. Mohammadi *et al.*, "Full-duplex non-orthogonal multiple access for next generation wireless systems," *IEEE Commun. Mag.*, vol. 57, no. 5, pp. 110–116, Apr. 2019.
- [24] C. Saha, M. Afshang, and H. Dhillon, "Integrated mmwave access and backhaul in 5G: Bandwidth partitioning and downlink analysis," 2017, *arXiv:1710.06255v1*. [Online]. Available: <https://arxiv.org/abs/1710.06255v1>
- [25] M. N. Kulkarni, A. Ghosh, and J. G. Andrews, "How many hops can self-backhauled millimeter wave cellular networks support?" 2018, *arXiv:1805.01040v2*. [Online]. Available: <https://arxiv.org/abs/1805.01040v2>
- [26] G. C. Alexandropoulos and M. Duarte, "Low complexity full duplex MIMO: Novel analog cancellation architectures and transceiver design," 2018, *arXiv:1809.09474v1*. [Online]. Available: <https://arxiv.org/abs/1809.09474v1>
- [27] Y.-B. Kim and W. Choi, "Interference cancelation based opportunistic relaying with multiple decode-and-forward relays," in *Proc. IEEE Veh. Technol. Conf.*, Ottawa, ON, Canada, Sep. 2010, pp. 1–5.
- [28] Y.-B. Kim, W. Choi, B. C. Jung, and A. Nosratinia, "A dynamic paradigm for spectrally efficient half-duplex multi-antenna relaying," *IEEE Trans. Wireless Commun.*, vol. 12, no. 9, pp. 4680–4691, Sep. 2013.
- [29] D. N. C. Tse and P. Viswanath, *Fundamentals of Wireless Communication*. Cambridge, U.K.: Cambridge Univ. Press, 2004.
- [30] D. N. C. Tse, P. Viswanath, and L. Zheng, "Diversity-multiplexing tradeoff in multiple-access channels," *IEEE Trans. Inf. Theory*, vol. 50, no. 9, pp. 1859–1874, Sep. 2004.
- [31] S. M. Ross, *Stochastic Process*, 2nd ed. Hoboken, NJ, USA: Wiley, 1996.
- [32] L. Zheng and D. N. C. Tse, "Diversity and multiplexing: A fundamental tradeoff in multiple-antenna channels," *IEEE Trans. Inf. Theory*, vol. 49, no. 5, pp. 1073–1096, May 2003.
- [33] H. Ebrahimzad and A. K. Khandani, "On diversity-multiplexing tradeoff of the interference channel," in *Proc. IEEE Int. Symp. Inf. Theory*, Seoul, South Korea, Jun./Jul. 2009, pp. 1614–1618.
- [34] H. Ebrahimzad and A. K. Khandani, "On the optimum diversity-multiplexing tradeoff of the two-user Gaussian interference channel with Rayleigh fading," *IEEE Trans. Inf. Theory*, vol. 58, no. 7, pp. 4481–4492, Jul. 2012.